Multiresolution-Based Image Fusion with Additive Wavelet Decomposition

Jorge Núñez, Xavier Otazu, Octavi Fors, Albert Prades, Vicenç Palà, and Román Arbiol

Abstract— **The standard data fusion methods may not be satisfactory to merge a high-resolution panchromatic image and a low-resolution multispectral image because they can distort the spectral characteristics of the multispectral data. In this paper, we developed a technique, based on multiresolution wavelet decomposition, for the merging and data fusion of such images. The method presented here consists of adding the wavelet coefficients of the high-resolution image to the multispectral (low-resolution) data. We have studied several possibilities concluding that the method which produces the best results consists in adding the high order coefficients of the wavelet transform of the panchromatic image to the intensity component (defined as $L = \frac{R+G+B}{3}$) of the multispectral image. The method is, thus, an improvement on standard intensity-hue-saturation (IHS or LHS) mergers. We used the "à trous" algorithm which allows to use a dyadic wavelet to merge nondyadic data in a simple and efficient scheme. We used the method to merge SPOT and LANDSAT (TM) images. The technique presented is clearly better than the IHS and LHS mergers in preserving both spectral and spatial information.**

I. INTRODUCTION

THERE ARE several situations that simultaneously require high spatial and high spectral resolution in a single image. This is particularly important in remote sensing. In other cases, such as astronomy, high spatial resolution and high signal-to-noise ratio (SNR) may be required. However, in most cases, instruments are not capable of providing such data either by design or because of observational constraints. For example, in remote sensing, SPOT PAN satellite provides high-resolution (10 m pixels) panchromatic data, while LANDSAT TM satellite data provides low-resolution (30 m pixels) multispectral images. In astronomy, the spaceborne telescopes give high-resolution images but the photons are expensive to collect, making long-exposure multispectral observations unusual. From the ground, on the other hand, the resolution is poor but the photons are cheap to collect and the SNR can be increased. Besides, it is easy to obtain long-exposure (but low-resolution) multispectral data from the ground.

One possible solution comes from the field of data fusion [1]. A number of methods have been proposed for merging panchromatic and multispectral data [2], [3]. The most common procedures are the intensity-hue-saturation transform based methods (IHS and LHS mergers) [4], [5]. However, the IHS and LHS methods produce spectral degradation. This is particularly crucial in remote sensing if the images to merge were not taken at the same time. In the last few years, multiresolution analysis has become one of the most promising methods for the the analysis of images in remote sensing [6]. Recently, several authors ([7]–[13]) proposed a new approach to image merging that uses a multiresolution analysis procedure based upon the discrete two-dimensional (2-D) wavelet transform. We also carried out a preliminary study of the wavelet-based method in combination with image reconstruction [14]. The wavelet approach preserves the spectral characteristics of the multispectral image better than the standard IHS or LHS methods.

Wavelet-based image merging can be performed in two ways: 1) by replacing some wavelet coefficients of the multispectral image by the corresponding coefficients of the high-resolution image and 2) by adding high-resolution coefficients to the multispectral data. Here, we further explore the wavelet transform image merging technique with special attention to the "additive" merger. To decompose the data into wavelet coefficients, we use the discrete wavelet transform algorithm known as "à trous" ("with holes"). The method is applied to merge SPOT and LANDSAT (TM) images.

II. STANDARD MERGING METHODS

The standard merging methods are based on the transformation of the RGB multispectral channels into the IHS components [15]. Intensity refers to the total color brightness, Hue refers to the dominant or average wavelength contributing to a color and Saturation refers to the purity of a color relative to gray. In the standard methods, the usual steps to perform are the following.

1) Register the low-resolution multispectral image to the same size as the high-resolution panchromatic image in order to be superimposed. Usually, the images are registered up to within 0.25 pixels rms resampling the LANDSAT data using control points and a bi-cubic polynomial fit.
2) Transform the R, G, and B bands of the multispectral image into the IHS components.
3) Modify the high-resolution panchromatic image to take into account the spectral differences with respect to the

multispectral image, the different atmospheric and illumination conditions, etc. This is usually performed by conventional histogram matching between the panchromatic image and the intensity component of the IHS representation. Specifically, after computing the histogram of both the panchromatic image and the Intensity component of the multispectral, the histogram of the Intensity (of the multispectral) is used as reference to which we match the histogram of the panchromatic image.

4) Replace the intensity component by the panchromatic image and perform the inverse transformation to obtain the merged RGB image with merged panchromatic information.

Throughout this paper we asume that all R, G, and B values are scaled over the range 0,255.

The result of the standard merging methods depends on the IHS system used. Many IHS transformation algorithms have been developed for converting the RGB values. While the complexity of the models varies, they produce similar values for hue and saturation. However, the algorithms differ in the method used in calculating the intensity component of the transformation. The most common intensity definitions are

$$I = \max(R, G, B)$$
$$L = \frac{R + G + B}{3}$$
$$L' = \frac{\max(R, G, B) + \min(R, G, B)}{2}.$$

We call the systems based on these definitions IHS, LHS, and L'HS color systems, respectively. The first system (based on I), also known as the Smith's hexcone [15], ignores two of the components to compute the intensity and will produce equal intensity for a pure color (e.g. 255, 0, 0) and for a white pixel (255, 255, 255). However, the second system (based on L), known as Smith's triangle model [15], would produce intensities of 255 for a white pixel but only 85 for a pure color. The third system (based on L') [16] would again produce a result of 255 for the white pixel, and 125 for a pure color.

Furthermore, the transformation algorithm based on the third definition (L') shows bizarre behavior in some cases. For example, if we have RGB values of (100, 150, 200), transform them to L'HS, add ten counts (over a maximum of 255) to the L' component and reverse the transformation, the resulting RGB values are (115, 160, 205), i.e., the color with the lowest value (R) is the one which has largest increment, while the component with highest value (B) has the lowest increment. On the other hand, if we transform the same RGB values (100, 150, 200) to the LHS sytem and again add 10 counts to the L component and reverse the transformation, the RGB values would be (107, 160, 213). In this case, the increment of ten counts in the intensity is distributed proportionally to the values of the R, G, and B components.

Thus, in this paper, we prefer the definition $L = \frac{R + G + B}{3}$ for the intensity component, although we will also use the definitions I and L', in the first example of Section V, to compare the results. The IHS and LHS methods will be also used to compare our results with the standard merging methods. When the intensity component is defined as L it is also called Lightness.

III. WAVELET DECOMPOSITION

Multiresolution analysis based on the wavelet theory permits the introduction of the concepts of details between successive levels of scale or resolution.

Wavelet decomposition is increasingly being used for the processing of images [17]–[24]. The method is based on the decomposition of the image into multiple channels based on their local frequency content. The wavelet transform provides a framework to decompose images into a number of new images, each one of them with a different degree of resolution. While the Fourier transform gives an idea of the frequency content in our image, the wavelet representation is an intermediate representation between the Fourier and the spatial representation, and it can provide good localization in both frequency and space domains. The wavelet transform of a distribution $f(t)$ can be expressed as

$$W(\mathbf{f})(a, b) = |a|^{-\frac{1}{2}} \int_{-\infty}^{+\infty} f(t) \, \psi\left(\frac{t - b}{a}\right) dt \qquad (1)$$

where a and b are scaling and translational parameters, respectively. Each base function $\psi(\frac{t-b}{a})$ is a scaled and translated version of a function ψ called *Mother Wavelet*. These base functions are $\int \psi(\frac{t-b}{a}) = 0$.

A. The "à trous" Algorithm

The discrete approach of the wavelet transform can be done with several different algorithms. However, not all algorithms are well suited for all the problems. The popular Mallat's algorithm [25] uses an orthonormal basis, but the transform is not shift-invariant, which can be a problem in signal analysis, pattern recognition or, as in our case, data fusion [22].

To obtain a shift-invariant discrete wavelet decomposition for images, we follow Starck and Murtagh [26], and we use the discrete wavelet transform known as "à trous" ("with holes") algorithm [27] to decompose the image into wavelet planes. Given an image $\mathbf{p}$ we construct the sequence of approximations:

$$F_1(\mathbf{p}) = \mathbf{p}_1, \quad F_2(\mathbf{p}_1) = \mathbf{p}_2, \quad F_3(\mathbf{p}_2) = \mathbf{p}_3, \quad \cdots.$$

To construct the sequence, this algorithm performs successive convolutions with a filter obtained from an auxiliary function named scaling function. We use a scaling function which has a $\mathbf{B}_3$ cubic spline profile. The use of a $\mathbf{B}_3$ cubic spline leads to a convolution with a mask of 5×5:

$$\frac{1}{256} \begin{pmatrix} 1 & 4 & 6 & 4 & 1 \\ 4 & 16 & 24 & 16 & 4 \\ 6 & 24 & 36 & 24 & 6 \\ 4 & 16 & 24 & 16 & 4 \\ 1 & 4 & 6 & 4 & 1 \end{pmatrix}. \qquad (2)$$

The wavelet planes are computed as the differences between two consecutive approximations $\mathbf{p}_{l-1}$ and $\mathbf{p}_l$. Letting $\mathbf{w}_l =$

$\mathbf{p}_{l-1} - \mathbf{p}_l$ $(l = 1, \ldots, n)$, in which $\mathbf{p}_0 = \mathbf{p}$, we can write the reconstruction formula

$$\mathbf{p} = \sum_{l=1}^{n} \mathbf{w}_l + \mathbf{p}_r. \qquad (3)$$

In this representation, the images $\mathbf{p}_l$ $(l = 0, \ldots, n)$ are versions of the original image $\mathbf{p}$ at increasing scales (decreasing resolution levels), $\mathbf{w}_l$ $(l = 1, \ldots, n)$ are the multiresolution wavelet planes, and $\mathbf{p}_r$ is a residual image. In our case, we are using a dyadic decomposition scheme. Thus, the original image $\mathbf{p}_0$ has double resolution than $\mathbf{p}_1$, the image $\mathbf{p}_1$ double resolution than $\mathbf{p}_2$, and so on. If the resolution of image $\mathbf{p}_0$ is, for example, 10 m, the resolution of $\mathbf{p}_1$ would be 20 m, the resolution of $\mathbf{p}_2$ would be 40 m, etc. Note, however, that all the consecutive approximations (and wavelet planes) in this process have the same number of pixels as the original image. This is a consequence of the fact that the "à trous" algorithm is a nonorthogonal oversampled transform [22]. This is a restriction on the use of this particular wavelet approach for applications such as image compression.

IV. WAVELET IMAGE FUSION METHOD

The wavelet merger method is based on the fact that, in the wavelet decomposition, the images $\mathbf{p}_l$ $(l = 0, \ldots, n)$ are the successive versions of the original image at increasing scales. Thus, the first wavelet planes of the high-resolution panchromatic image have spatial information that is not present in the multispectral image. The wavelet-based image merging can be carried out in two ways, as follows.

A. Substitution Method

In the wavelet substitution method, some of the wavelet planes of the multispectral image are substituted by the planes corresponding to the panchromatic image as follows.

1) Register, as in Section II, the low-resolution multispectral image to the same size as the high-resolution panchromatic image in order to be superimposed.
2) Perform histogram matching between the panchromatic image and the intensity component of the color image as before. Let **PAN** be the panchromatic image and **R**, **G**, and **B** be the three bands of the multispectral image.
3) Decompose the R, G, and B bands of the multispectral image to n wavelet planes (resolution levels). Usually $n = 2 \ or \ 3$.

$$\mathbf{R} = \sum_{l=1}^{n} \mathbf{w}_{\mathbf{R}l} + \mathbf{R}_r$$

$$\mathbf{G} = \sum_{l=1}^{n} \mathbf{w}_{\mathbf{G}l} + \mathbf{G}_r$$

$$\mathbf{B} = \sum_{l=1}^{n} \mathbf{w}_{\mathbf{B}l} + \mathbf{B}_r.$$

4) Decompose the panchromatic high-resolution image accordingly.

$$\mathbf{PAN} = \sum_{l=1}^{n} \mathbf{w}_{\mathbf{P}l} + \mathbf{PAN}_r.$$

5) Replace the first wavelet planes of the R, G and B decompositions by the equivalent planes of the panchromatic decomposition.
6) Perform the inverse wavelet transform.

$$\mathbf{R}_{\mathrm{new}} = \sum_{l=1}^{n} \mathbf{w}_{\mathbf{P}l} + \mathbf{R}_r$$

$$\mathbf{G}_{\mathrm{new}} = \sum_{l=1}^{n} \mathbf{w}_{\mathbf{P}l} + \mathbf{G}_r$$

$$\mathbf{B}_{\mathrm{new}} = \sum_{l=1}^{n} \mathbf{w}_{\mathbf{P}l} + \mathbf{B}_r.$$

B. Additive Method

Another possibility is to add the wavelet planes of the high-resolution image directly to the multispectral image. The steps of this "additive" method are the following.

1) Adding to the RGB Components: The first possibility [8] is to add the high-resolution information directly to the R, G, and B bands. The steps of the method are as follows.

1) Register the low-resolution multispectral image and perform histogram matching between the panchromatic image and the intensity component of the color image as before. Let **PAN** be the panchromatic image and **R**, **G**, and **B** be the three bands of the multispectral image.
2) Decompose only the panchromatic high-resolution image to n wavelet planes (resolution levels). Usually, $n = 2 \ or \ 3$.

$$\mathbf{PAN} = \sum_{l=1}^{n} \mathbf{w}_{\mathbf{P}l} + \mathbf{PAN}_r.$$

3) Add the wavelet planes of the panchromatic decomposition to the R, G, and B bands of the multispectral image.

$$\mathbf{R}_{\mathrm{new}} = \sum_{l=1}^{n} \mathbf{w}_{\mathbf{P}l} + \mathbf{R}$$

$$\mathbf{G}_{\mathrm{new}} = \sum_{l=1}^{n} \mathbf{w}_{\mathbf{P}l} + \mathbf{G}$$

$$\mathbf{B}_{\mathrm{new}} = \sum_{l=1}^{n} \mathbf{w}_{\mathbf{P}l} + \mathbf{B}.$$

We call this method AWRGB.

2) Adding to the Intensity Component: Another possibility, which we consider the best approach, is to incorporate the high-resolution information directly to the intensity component of the multispectral image. We carried out a preliminary study of this approach [28], [29]. The steps of the method are the following.

Steps 1) and 2) are as before. Thus

$$\mathbf{PAN} = \sum_{l=1}^{n} \mathbf{w}_{\mathbf{P}l} + \mathbf{PAN}_r.$$

3) Transform the RGB components of the multispectral image into the IHS representation. Let **L**, **H** and **S**, be the three componets of the multispectral image.

4) Add the wavelet planes of the panchromatic decomposition to the **L** component.

$$\mathbf{L}_{\mathrm{new}} = \sum_{l=1}^{n} \mathbf{w}_{\mathbf{P}\,l} + \mathbf{L}$$

5) Transform the new values back into RGB representation.

As stated above, we can use I, L, and L′ to represent the intensity component. Depending on which of the intensity definition is used we call the merging method AWI, AWL, and AWL′, respectively. However, as stated in Section II, we will prefer to use use $L = \frac{R+G+B}{3}$ (AWL method) to represent the intensity component.

In the substitution method, the wavelet planes corresponding to the multispectral image are discarded and substituted by the corresponding planes of the panchromatic image. However, in the additive method all the spatial information in the multispectral image is preserved. Thus, the main advantage of the additive method is that the detail information from both sensors is used. The main difference between adding the panchromatic wavelet planes to the R, G, and B bands or to the intensity component is that in the first case, panchromatic information is added in the same amount to all three bands, biasing the color of the pixel toward the gray, while in the second case the high-resolution information modifies only the intensity, preserving multispectral information in a better way. Thus, from the theoretical point of view, adding to the intensity component is a better choice than adding to the R, G, and B bands. As stated in Section II, the reason for using the L component to represent the intensity instead of using I or L′ is that I ignores two of the RGB values, and, using L′, the increments of intensity (obtained by adding the wavelet planes) are distributed, in some cases, not proportionally to the RGB values.

The advantages of using the wavelet image merging technique over the standard IHS or LHS methods are as follows.

1) The spectral quality of the color image is preserved to a higher degree.
2) The resolution of the panchromatic image is added to the solution without discarding the resolution of the multispectral image. Thus, the detail information from both images is used.
3) The wavelet planes (except the residual image) have zero mean. Thus, the total flux of the multispectral image is preserved.
4) The additive wavelet on the intensity method can be considered as an improvement on the classical IHS/LHS method in the sense that the intensity component is not substituted by the panchromatic image, but the highest resolution features not present in the multispectral image are introduced into the merged image by adding the first wavelet planes of the panchromatic image to the intensity component.

It is important to note that the AWL method allows use of a dyadic wavelet ("à trous") to merge nondyadic data as, for example, LANDSAT (30 m) images and SPOT (10 m) images.

Is interesting to note that our wavelet image fusion method have similarities but also differences with the ARSIS method [10]. The ARSIS method consists in to perform a wavelet transform on a high-resolution image using an image pyramid similar to the Laplace pyramid [30], replace then the first signal approximation which has half the initial resolution with images from a multispectral data set, and perform the inverse wavelet transform. Since the "à trous" algorithm also uses a dyadic decomposition (but without the decimating which gives the pyramidal scheme), our AWRGB method (not the AWL that adds on the L component) would almost coincide with ARSIS if the data were dyadic (as, for example, SPOT-XS and SPOT-P) and only one wavelet plane were added. There is a nondyadic ARSIS extension [13] that uses a "tryadic" wavelet to merge SPOT and LANDSAT images but it is needed to devise a different wavelet for each resolution ratio. As stated above, our wavelet image fusion methods (AWRGB, AWL) give a simple and efficient solution using always the same dyadic wavelet to merge images of any resolution.

V. RESULTS

We applied the above methodology to merge SPOT and a LANDSAT (TM) images. The original panchromatic SPOT images have 10-m pixels while the original multispectral LANDSAT (TM) images have 30-m pixels. The LANDSAT original bands were converted to the (R, G, B) system using the following transformation: $R = \frac{B_5+B_7}{2}$, $G = \frac{B_3+B_4}{2}$, $B = \frac{B_1+B_2}{2}$. We present two examples in the following subsections. The first example is a low resolution image generated to have an original image to which compare the results. The aim of this first example is to quantify the gain of the different merging methods. The second example shows the application of our preferred method to a full-resolution image.

A. Application to an Inferior Level

Because we do not have any LANDSAT (multispectral) image at 10-m resolution to compare with, the evaluation of the improvement of the additive wavelet method with respect to other merging methods is not easy. To solve this problem, in the first example, we applied the merging method to an inferior level of resolution, that is to say, on a SPOT panchromatic image at 30-m resolution and a LANDSAT multispectral image at 90-m resolution. The result of the image fusion method is a merged multispectral image at 30-m resolution which can be compared with the original LANDSAT image at 30 m. In this first example, we use a scene that includes both urban area and agricultural lots. The SPOT and LANDSAT images were taken at different epochs. This is an aditional problem for the merging process but we chose this example because it is the usual case when the images to merge come from different satellites. We do not show the images of this lower resolution example to save space for the second example which is at full resolution.

The available SPOT and LANDSAT (TM) original images were degraded to 30-m and 90-m resolution, respectively. These degraded images are the images to merge. The images were registered and the SPOT image was photometrically corrected to present a histogram similar to the intensity component of the LANDSAT (TM) image. In order to compare the results, in this example we used the three definitions (I, L, L′) for the intensity component. Then, we applied the additive wavelet-based image fusion methods explained

TABLE I

CORRELATION BETWEEN THE STANDARD METHODS (IHS, L′HS, LHS), AND ADDITIVE WAVELET-BASED METHODS (AWRGB, AWI, AWL′, AWL) AND THE ORIGINAL LANDSAT TEMATIC MAPPER IMAGE AT 30-m RESOLUTION (TM$_{\text{orig.}}$)

Images	Correlation		
	Red	Green	Blue
$IHS/TM_{\text{orig.}}$	0.420	0.307	0.358
$L'HS/TM_{\text{orig.}}$	0.589	0.375	0.376
$LHS/TM_{\text{orig.}}$	0.668	0.376	0.421
$AWRGB/TM_{\text{orig.}}$	0.861	0.719	0.757
$AWI/TM_{\text{orig.}}$	0.805	0.639	0.711
$AWL'/TM_{\text{orig.}}$	0.836	0.695	0.759
$AWL/TM_{\text{orig.}}$	0.849	0.721	0.781
AWL'	Ditto, but adding to L' component		
AWL	Ditto, but adding to L component		

above (AWRGB, AWI, AWL, AWL′) and compared the results between them and to those given by the standard methods. In this example, three wavelet planes were added.

To quantify the behavior of the standard and wavelet-based image fusion methods we computed the correlation between the different solutions and the original LANDSAT at 30-m resolution image. To compute the correlation coefficient, we use the standard coefficient

$$Corr(A/B) = \frac{\sum_{j=1}^{\text{npix}}(A_j - \bar{A})(B_j - \bar{B})}{\sqrt{\sum_{j=1}^{\text{npix}}(A_j - \bar{A})\sum_{j=1}^{\text{npix}}(B_j - \bar{B})}}$$

where $\bar{A}$ and $\bar{B}$ state for the mean value of the corresponding data set.

Table I shows the correlations between the different solutions and the original LANDSAT (TM) at 30-m resolution image. As stated above, the different solutions are as follows.

IHS Standard substitution technique using I to represent the intensity.

L′HS Ditto, but using L′.

LHS Ditto, but using L.

AWRGB Additive wavelets solution adding the high-resolution information to the R, G and B bands.

AWI Additive wavelets solution adding the high-resolution information to the I component.

AWL′ Ditto, but adding to L′ component.

AWL Ditto, but adding to L component.

The first, second, and third lines of Table I show the correlation between the R, G, and B bands of the standard solutions (IHS, L′HS, LHS) and the same bands of the original LANDSAT (TM) at 30 m resolution. Note that the best solution between the standard methods corresponds to the LHS method as expected from the theory exposed in Section II.

The last four lines of Table I show the correlation between the R, G, and B bands of the additive wavelet-based solutions (AWRGB, AWI, AWL′, and AWL) and the same bands of the original LANDSAT (TM) at 30-m resolution. Note that the correlations of all the additive wavelet-based solutions are clearly higher than the correlations of the standard solutions. This means that the additive wavelet solutions preserve the spectral characteristics of the multispectral image to a greater extent than the standard IHS, L′HS, and LHS solutions.

Fig. 1.   Detail of the SPOT image.

Looking to the correlations of the additive wavelet solutions, we can see that the correlations obtained for the AWL solution are higher than the AWI and AWL′ methods. This is, again, in accordance with the theory that the L component represents the intensity component better that I or L′ (Section II). The correlations of the AWRGB solution are very close to the correlations of the AWL method. Note that the correlation in the R band is even higher in AWRGB than in AWL, although this is compensated by the higher value of the correlation of the AWL in B band. However, as stated above, from the theoretical point of view, adding to the L component (AWL) is a better choice than adding to the R, G, and B bands (AWRGB) because the last introduces a bias in the color of the pixel toward the gray.

Regarding to the degree of correlation obtained, although the target would be a correlation of 1.0 (perfect reconstruction of the original image), given that the LANDSAT and SPOT images were taken at different epochs this is not possible. Correlations of about 0.85 as the ones obtained with the additive wavelet method should be considered as the maximum correlation possible in this case.

Thus, the main conclusion of this section is that the additive wavelet solution on L (AWL) behaves better than the standard methods and the other additive wavelet-based methods in preserving both spatial and spectral characteristics of the original image during the image merging process. This is our preferred method, which will be used to merge the images at full resolution of the following example.

B. Application to Full Resolution

In the second example, we merge two SPOT and LANDSAT images at their full resolution. As stated above, the original SPOT image has 10-m pixels, while the LANDSAT image has 30-m pixels. The images show a small portion of the Argentinian coast that includes urban area, agricultural lots
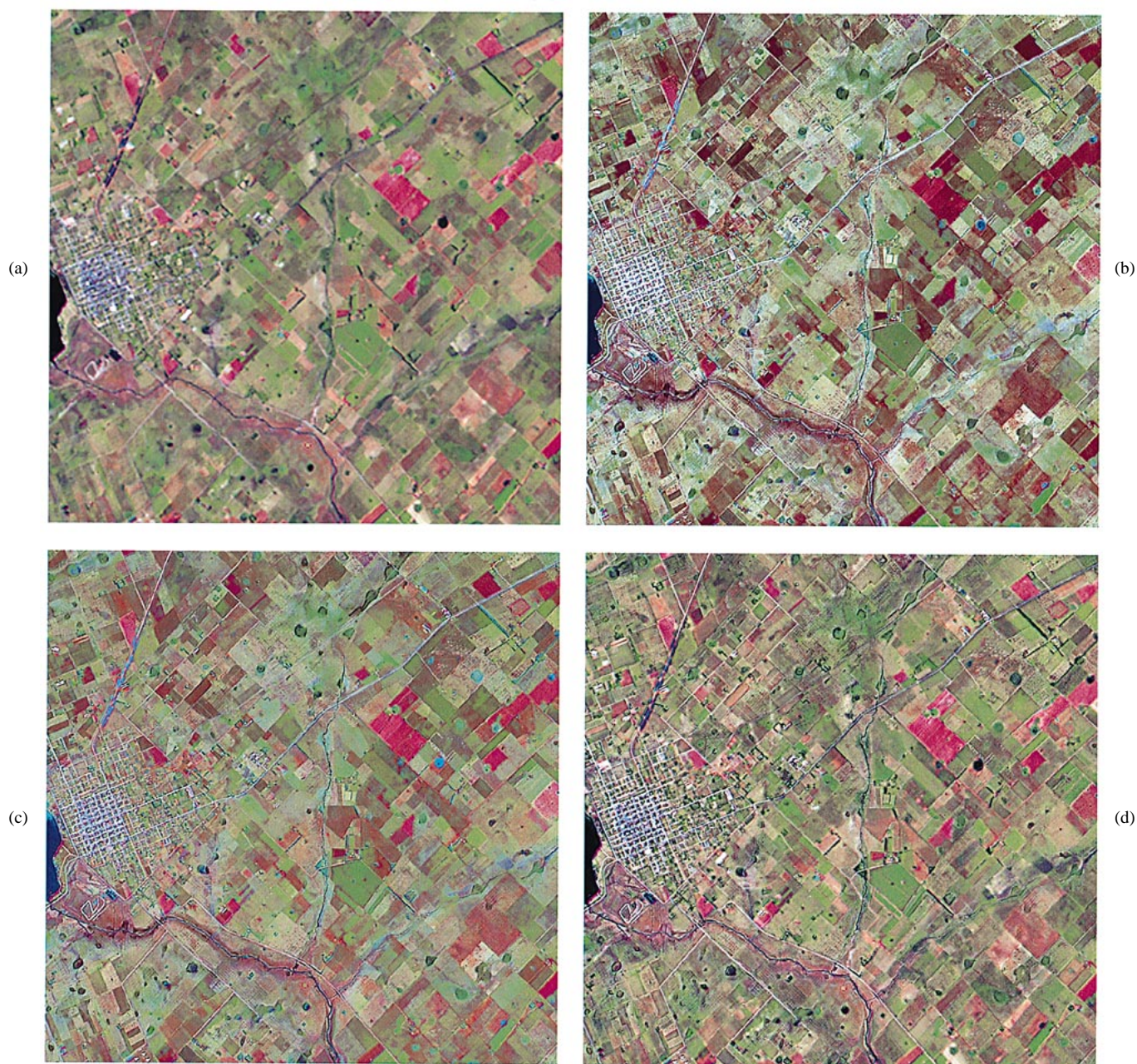
Fig. 2. (a) Detail of the LANDSAT (TM) image. (b) Result of the fusion by the standard IHS method. (c) Result of the fusion by the standard LHS method. (d) Result of the fusion by the additive wavelets on L component (AWL) method.

and rivers. The images were registered and the SPOT image was photometrically corrected to present a histogram similar to the L component of the LANDSAT image. Then, we applied the AWL image fusion technique and compared the results to those given by the standard methods.

Fig. 1 shows a detail of the original SPOT image. Fig. 2(a) shows the same area of the LANDSAT image. The spatial resolution of the SPOT image is clearly better than the LANDSAT image as expected from the different pixel size. It is easy to see that the SPOT and LANDSAT images were taken at different epochs, as is usual when working with images from different satellites. Note, for example, the aspect of the bed of the river, the water ponds (black rounded areas in the SPOT image) or the crop fields, which in the SPOT image are clearly

different from their appearance in the LANDSAT image. Also, there are several structures in the SPOT picture that were not present when the LANDSAT image was taken.

Fig. 2(b) shows the result of the fusion of the LANDSAT and SPOT images by the standard IHS method. The increase in resolution with respect to the original LANDSAT image is evident. Most of the resolution of the SPOT image has been incorporated into the result. However, as stated above, there is spectral degradation and intensity dependence of the resulting color and a strong correlation between the merged image and the panchromatic intensity. This fact can be seen qualitatively in the colors of the crop fields, in the streets of the city, or the bed of the river at the bottom of the image, in comparison with the same areas in Fig. 2(a). Fig. 2(c) shows the fusion of the

TABLE II
CORRELATION BETWEEN IHS, LHS AND ADDITIVE WAVELETS ON L COMPONENT
(AWL) MERGING METHODS AND SPOT AND LANDSAT (TM) IMAGES

	Correlation		
Images	Red	Green	Blue
$TM/SPOT$	0.191	0.149	0.313
$IHS/SPOT$	0.911	0.734	0.830
$LHS/SPOT$	0.758	0.734	0.774
$AWL/SPOT$	0.487	0.608	0.724
IHS/TM	0.418	0.338	0.121
LHS/TM	0.722	0.399	0.117
AWL/TM	0.923	0.801	0.740

same images using the standard LHS method. Here, the colors of the fields in the image match better the corresponding colors of Fig. 2(a), but note, for example, the blue color of the water beside the city (black in the LANDSAT image) as in other areas. Note, also, the aspect of the bed of the river or the streets of the city, which are similar to those of the IHS result.

Fig. 2(d) shows the result of the fusion by the additive wavelet on L (AWL) method. In this example, three wavelet planes were added. As in the IHS/LHS solution, most of the resolution of the SPOT image was incorporated to the merged image. However, in this case, the spectral characteristics of the LANDSAT image are preserved better than in the standard mergers. Note the nearly identical tonalities of Figs. 2(d) and (a). In particular, the water beside the city is black as in the LANDSAT image, the bed of the river has the same appearance as in Fig. 2(a), and the streets of the city are better delineated than in the standard results.

In this example, we do not have any original image (LANDSAT at 10 m pixels) to compare with. However, we can quantify, in some way, the behavior of the AWL method in comparison with the standard methods by computing the correlation of the IHS, LHS, and AWL solutions with regard to the SPOT and LANDSAT images. Note that in this case, the target for the correlation is not 1.0. Also, a higher correlation with SPOT does not mean a better result. Note, also, that the correlation between images of different resolution (as the correlation between the TM image and the fused images) has no intrinsic significance, but it can be used to compare the behavior of the different solutions.

Table II shows the correlations between the solutions by the IHS, LHS, and AWL merging methods and the original LANDSAT and SPOT images. The first line of Table II shows the correlation between the R, G, and B bands of the LANDSAT (TM) image and the SPOT image. The second and third lines show the correlation between the R, G, and B bands of the IHS and LHS solutions and the SPOT. The fourth line shows the correlations of the AWL solution. Note that the correlations of the IHS and LHS solutions are higher (especially in R) than the correlations of the AWL solution. This means that the standard solutions are closer to the SPOT image than the AWL solution. However, this is not a weakness of the AWL method. As stated above, there is strong correlation between the IHS and LHS merged images and the intensity of the panchromatic image. This "too high" correlation produces solutions that are closer to the SPOT image than desirable. The correlation is,

however, lower in the additive wavelets solution. This is a positive fact because it means a lower dependence of the AWL solution on the SPOT image.

Rows five to seven on Table II indicate the correlation between the same solutions and the LANDSAT (TM) image. Note that the correlation of our AWL solution is higher than of the IHS and LHS merging methods. This means that as stated above in qualitative terms, the additive wavelet solution on L preserves the spectral characteristics of the multispectral image to a greater extent than the IHS and LHS solutions. Thus, the additive wavelet solution on L behaves better than the standard methods.

VI. CONCLUSION

The additive wavelet-based methods are better suited for image merging than the standard techniques based on component substitution. These methods combine a high-resolution panchromatic image and a low-resolution multispectral image by adding some wavelet planes of the panchromatic image to the intensity component of the low-resolution image. The use of the "à trous" algorithm allows to use a dyadic wavelet to merge nondyadic data as, for example, LANDSAT (30 m) images and SPOT (10 m) images in a simple and efficient scheme. Between the different wavelet-based methods studied, the additive wavelet method on the L component defined as $L = \frac{R+G+B}{3}$ (AWL), performs better. Using this method, the detail information from both images is preserved. The method is capable of enhancing the spatial quality of the multispectral image while preserving its spectral content to a greater extent. The AWL method does not modify the total flux of the multispectral image since the mean value of each of the added wavelet planes is 0. The AWL method can be considered as an improvement on the classical IHS or LHS methods in the sense that the intensity is not substituted by the panchromatic image but the high-resolution of the panchromatic image is injected into the merged image by the addition of some wavelet planes of the panchromatic image to the intensity component of the multispectral low-resolution image.

REFERENCES

[1] T. Taxt and A. H. Schistad-Solberg, "Data fusion in remote sensing," in *Fifth Workshop on Data Analysis in Astronomy*, V. Di Gesu and L. Scarsi, Eds., Erice, Italy, Nov. 1996.
[2] P. S. Chavez, S. C. Sides, and J. A. Anderson, "Comparison of three different methods to merge multi-resolution and multispectral data: Landsat TM and SPOT panchromatic," *Photogramm. Eng. Remote Sensing*, vol. 57, no. 3, pp. 295–303, 1991.
[3] J. C. Tilton, Ed., *Multisource Data Integration in Remote Sensing*, NASA Conf. Publ., 1991, vol. 3099.
[4] J. W. Carper, T. M. Lillesand, and R. W. Kiefer, "The use of intensity-hue-saturation transformations for merging SPOT panchromatic and multispectral image data," *Photogramm. Eng. Remote Sensing*, vol. 56, pp. 459–467, 1990.
[5] V. K. Shettigara, "A Generalized component substitition technique for spatial enhacement of multispectral images using a higher resolution data set," *Photogramm. Eng. Remote Sensing*, vol. 58, pp. 561–567, 1992.
[6] M. Datcu, D. Luca, and K. Seidel, "Multiresolution analysis of SAR images," in *Proc. EUSAR'96*, Konigswinter, Germany, pp. 375–378, 1996.
[7] D. A. Yocky, "Image merging and data fusion by means of the discrete two-dimensional wavelet transform," *J. Opt. Soc. Amer. A*, vol. 12, no. 9, pp. 1834–1841, 1995.

[8] ——, "Multiresolution wavelet decomposition image merger of LANDSAT thematic mapper and SPOT panchromatic data," *Photogramm. Eng. Remote Sensing*, vol. 62, no. 9, pp. 1067–1074, 1996.

[9] B. Garguet-Duport, J. Girel, J. M. Chassery, and G. Pautou, "The use of multiresolution analysis and wavelets transform for merging SPOT panchromatic and multispectral image data," *Photogramm. Eng. Remote Sensing*, vol. 62, no. 9, pp. 1057–1066, 1996.

[10] T. Ranchin, L. Wald, and M. Mangolini, "The ARSIS method: A general solution for improving spatial resolution of images by the means of sensor fusion," in *Proc. Int. Conf. Fusion of Earth Data*, T. Ranchin and L. Wald, Eds., Cannes, France, 1996, pp. 53–58.

[11] L. Wald, T. Ranchin, and M. Mangolini, "Fusion of satellite images of different spatial resolution: Assessing the quality of resulting images," *Photogramm. Eng. Remote Sensing*, vol. 63, no. 6, pp. 691–699, 1997.

[12] J. Zhou, D. L. Civco, and J. A. Silander, "A wavelet transform method to merge Landsat TM and SPOT panchromatic data," *Int. J. Remote Sensing*, vol. 19, no. 4, pp. 743–757, 1998.

[13] P. Blanc, T. Blu, T. Ranchin, L. Wald, and R. Aloisi, "Using iterated rational filter banks within the ARSIS concept for producing 10 m LANDSAT multispectral images," *Int. J. Remote Sensing*, vol. 19, no. 12, pp. 2331–2343, 1998.

[14] J. Núñez, X. Otazu, O. Fors, and A. Prades, "Simultaneous image fusion and reconstruction using wavelets. Applications to SPOT + LANDSAT images," *Vistas Astron.*, vol. 41, no. 3 pp. 351–357, 1997.

[15] A. R. Smith, "Color gamut transform pairs," *Comput. Graph.*, vol. 12, pp. 12–19, 1978.

[16] Association for Computing Machinery (ACM), "Status report of the graphics standard planning committee," *Comput. Graph.*, vol. 13, no. 3, 1979.

[17] Y. Meyer, *Wavelets. Algorithms and Applications*. Philadelphia, PA: SIAM, 1993.

[18] R. K. Young, *Wavelet Theory and Its Applications*. Boston, MA: Kluwer, 1993.

[19] I. Daubechies, *Ten Lectures on Wavelets*. Philadelphia, PA: SIAM, 1992.

[20] C. K. Chui, *An Introduction to Wavelets*. Boston, MA: Kluwer, 1992.

[21] G. Kaiser, *A Friendly Guide to Wavelets*. Boston, MA: Birkhauser, 1994.

[22] M. Vetterli and J. Kovacevic, *Wavelets and Subband Coding*. Englewood Cliffs, NJ: Prentice-Hall, 1995.

[23] J. L. Starck and E. Pantin, "Multiscale maximum entropy image restoration," *Vistas Astron.*, vol. 40, pp. 563–569, 1996.

[24] F. Rué and A. Bijaoui, "A multiscale vision model applied to astronomical images," *Vistas Astron.*, vol. 40, pp. 495–502, 1996.

[25] S. Mallat, "A theory for multiresolution signal: The wavelet representation," *IEEE Trans. Pattern Anal. Machine Intell.*, vol. 11, July 1989.

[26] J. L. Starck and F. Murtagh, "Image restoration with noise suppression using the wavelet transform," *Astron. Astrophys.*, vol. 288, pp. 342–350, 1994.

[27] M. Holschneider and P. Tchamitchian, *Les Ondelettes en 1989*, P.G. Lemarié, Ed. Paris, France: Springer-Verlag, 1990, p. 102.

[28] J. Núñez, X. Otazu, O. Fors, and A. Prades, "Fusion and reconstruction of LANDSAT and SPOT images using wavelets," in *Proc. Fusion of Earth Data*, T. Ranchin and L. Wald, Eds., Sophia Antipolis, France, Jan. 1998, pp. 103–108.

[29] J. Núñez, X. Otazu, O. Fors, A. Prades, V. Palá, and R. Arbiol, "Image fusion using additive multiresolution wavelet decomposition. Applications to SPOT + LANDSAT Images," *J. Opt. Soc. Amer. A*, vol. 16, no. 3, pp. 467–474, 1999.

[30] P. J. Burt and E. H. Adelson, "The Laplacian pyramid as a compact image code," *IEEE Trans. Commun.*, vol. COMM-31, pp. 532–540, Apr. 1983.

Xavier Otazu received the degree in physics from the University of Barcelona (UB), Spain, in 1994 and the M.Th. degree in 1996. He is now pursuing the Ph.D. degree in the Astronomy Department of UB on the applications of wavelets to astronomical data processing.

He is presently working at the Cartographic Institute of Catalonia, Spain, applying image processing techniques to remote sensing problems.

Octavi Fors received the degree in physics from the University of Barcelona (UB), Spain, in 1996.

He has since been working on astronomical image processing, first as a fellow at the Fabra Observatory and now in the Astronomy Department at UB with a predoctoral research staff formation fellowship. He also has been working in collaboration with the Cartographic Institute of Catalonia, Spain, applying image processing techniques to remote sensing problems.

Albert Prades received the degree in physics from the University of Barcelona, Spain, in 1992.

He has been working on image reconstruction techniques for remote sensing applications in collaboration with the Cartographic Institute of Catalonia. Presently, he is working on image restoration for astrometry. He is also an Assistant Professor at the Universitat Politecnica de Catalunya.
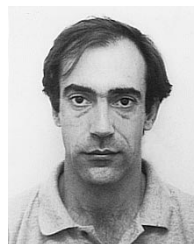
Vicenç Palà received the B.Eng. degree in computer science from the Universitat Politècnica de Catalunya (UPC), Spain, in 1984.

From 1982 to 1986, he was a Researcher at the UPC Computing Center, developing digital processing tools in the remote sensing domain. Since 1987, he has been working as Head of Image Processing and Systems Development, Cartographic Institute of Catalonia, where he is currently involved in projects related to image processing and geocoding.

Jorge Núñez received the B.A. degree in physics from the University of Barcelona, Spain, in 1975 and the Ph.D. in physics from the same university in 1981.

Since 1984, he has been a Professor in the Department of Astronomy, University of Barcelona. He is conducting research on digital image processing including image reconstruction and restoration using Bayesian techniques and data fusion with applications in astronomy, medicine, and remote sensing.

Román Arbiol received the B.S. degrees in physics from the University of Barcelona, Spain, in 1976, and in computer science from the Polytechnic University of Catalonia, Spain, in 1984.

Since 1980, he has been involved in the development of image processing algorithms to extract information from Earth observation satellite images. Since 1983, he has been the Head of the Image Processing and Remote Sensing Department, Cartographic Institute of Catalonia. His interest includes image restoration, image classification and geometrical models.